

## K-shell excitation of D<sub>2</sub>O and H<sub>2</sub>O ice: Photoion and photoelectron yields

R. A. Rosenberg,\* P. R. LaRoe, and Victor Rehn

*Michelson Laboratories, Naval Weapons Center, China Lake, California 93555*

J. Stöhr and R. Jaeger†

*Corporate Research Science Laboratories, Exxon Research and Engineering Company, Linden, New Jersey 07036*

C. C. Parks

*Lawrence Berkeley Laboratory and Department of Chemistry, University of California, Berkeley, Berkeley, California 94720*

(Received 7 April 1983)

The yield of photoelectrons and photoions from condensed H<sub>2</sub>O and D<sub>2</sub>O ice near and above the oxygen *K* edge is reported. Results of studies in the near-edge region indicate that Rydberg excitations, which are quenched in the bulk, survive, to some extent, on the surface. Analysis of the extended x-ray absorption fine structure of the photoelectron yield above the edge yields an oxygen-oxygen scattering phase shift in good agreement with theory.

### I. INTRODUCTION

Studies of the near-edge x-ray absorption fine structure (NEXAFS) (Refs. 1 and 2) and extended x-ray absorption fine structure (EXAFS) (Ref. 3) have been shown to yield unique chemical and structural information. Both EXAFS and NEXAFS structures arise from scattering processes of the excited photoelectron. In the better-understood and simpler-to-interpret EXAFS range the oscillations in the absorption coefficient result from the backscattering of energetic ( $\geq 50$  eV) photoelectrons by neighbor atoms. Because of their relatively high kinetic energy the photoelectrons predominantly scatter off the atomic cores. The EXAFS structure is therefore determined by the crystallographic arrangement (nuclear positions) of the neighbor atoms around the absorbing central atom. The details of the valence-electron distribution (bonding) have only a negligibly small effect on the EXAFS structure. The NEXAFS structure, on the other hand, arises from the scattering of low-energy ( $\leq 50$  eV) photoelectrons which are more sensitive to the valence-electron charge distribution. In general, the interpretation of the NEXAFS structure is therefore more complicated since multiple scattering effects need to be taken into account.

One case where the NEXAFS structure can readily be interpreted is that of a chemisorbed molecule on a surface. Previous NEXAFS studies<sup>1</sup> at the *K* absorption thresholds of chemisorbed diatomic low-*Z* molecules surprisingly showed little effect of the crystallographic arrangement of the substrate atoms and the chemisorption bonding (except for fixing the molecular orientation) but instead were dominated by similar absorption resonances as for the isolated (gas-phase) molecules.<sup>4</sup> The observed *intramolecular* resonances typically result from transitions to partially filled or empty molecular orbitals (bound-state resonances) or to continuum states with a large scattering amplitude near the molecule (shape resonances). It has been shown that the polarization dependence of the resonance intensities and their energy position relative to that observed in

the gas phase can provide valuable information on the molecular orientation, the charge transfer upon chemisorption, and the intramolecular bond length.

Here we address the case of a *molecular solid*, i.e., H<sub>2</sub>O ice, where individual molecular units are bonded together via hydrogen bridges. Since the EXAFS signal originates from scattering of the excited photoelectron by the cores of neighbor atoms it is not sensitive to the light hydrogen atoms but will reflect the distances and coordination of the heavier atoms in the matrix (i.e., oxygen). The NEXAFS signal on the other hand may still be reminiscent of that of the isolated molecule with perturbations induced by the intermolecular bonding. It is the goal of this paper to elucidate these perturbations by presenting NEXAFS spectra of H<sub>2</sub>O ice recorded by total-electron-yield (TY) detection and by means of the photon-stimulated ion desorption (PSID) technique.<sup>5</sup> In addition, we will use the measured EXAFS signal to determine the O-O scattering phase shift which can then be compared to published calculations.

The electronic structure of the various phases of ice has been investigated by a variety of techniques.<sup>6-16</sup> The valence-band structure has been studied by photoabsorption spectroscopy,<sup>6,7</sup> ultraviolet photoelectron spectroscopy (UPS),<sup>7,8</sup> and PSID.<sup>9</sup> X-ray photoelectron spectroscopy (XPS) (Refs. 7, 10, and 11) and Auger electron spectroscopy<sup>12</sup> have been utilized to study the core levels. Theoretical efforts have been limited to a calculation of the band structure of cubic ice.<sup>13</sup> A general review of electron- and photon-stimulated desorption processes has recently been published.<sup>14</sup> In this work an explanation of the electronic states involved in the valence-level PSID of ice was proposed<sup>15</sup> and preliminary findings of *K*-shell excitation of ice was presented.<sup>16</sup>

NEXAFS studies of ice were carried out by total electron yield (TY) and H<sup>+</sup> or D<sup>+</sup> ion yield detection. Because of the large (50 Å) escape depth of the inelastically scattered electrons (which dominate the TY signal) the TY NEXAFS spectra are representative of the bulk structure of the film. The PSID signal is sensitive to the outermost

surface layer of the molecular ice film. Our studies show that the Rydberg excitations observed in the *K*-shell excitation of water molecules in the gas phase<sup>17</sup> are severely perturbed and broadened in the solid due to the interaction between hydrogen atoms on different water molecules. The reduced coordination of the water molecules on the ice surface allows the lowest-lying Rydberg excitation to survive.

EXAFS spectra are capable of yielding bond distances even in the absence of long-range order. In the case of amorphous ice these distances are well known,<sup>18</sup> which affords the possibility of determining accurate oxygen-oxygen scattering phase shifts and amplitudes.<sup>19–21</sup> Calculations have been performed by Teo and Lee to determine EXAFS phase shifts and amplitudes.<sup>22</sup> These calculations have proven highly successful in interpreting EXAFS spectra of high-*Z* atoms.<sup>23</sup> However, results for low-*Z* atoms have indicated that the theoretical values are less accurate for these species.<sup>24</sup>

This discrepancy is not altogether unexpected because of the larger relative number of valence electrons for low-*Z* atoms. In the phase-shift calculations, chemical effects arising from different valence-electron configurations are neglected because the scattering is assumed to be dominated by the core-electron potential. For intermediate- and high-*Z* atoms this is a good approximation but for light elements such as oxygen it may be expected that the valence electrons influence the scattering potential on the absorbing atom as well as on the backscattering neighbor atom. Indeed, previous bulk EXAFS studies on oxides of semiconductors and metals in some cases indicated discrepancies between experimentally and theoretically derived phase shifts.<sup>24</sup> For H<sub>2</sub>O ice we find an oxygen-oxygen phase shift which is in surprisingly good agreement with the calculation of Teo and Lee.<sup>22</sup>

## II. EXPERIMENTAL

The experiments were performed at the Stanford Synchrotron Radiation Laboratory (SSRL) using two different ultrahigh vacuum chambers and two separate beam lines. TY and PSID NEXAFS and EXAFS of D<sub>2</sub>O ice condensed at 20 K were performed using apparatus 1. Similar measurements on H<sub>2</sub>O ice condensed at 90 K were carried out in apparatus 2. Water condensed below 123 K is expected to yield amorphous ice.<sup>18</sup>

Experiments with apparatus 1 were performed on SSRL beam line III-1 which employs a “grasshopper” monochromator with interchangeable gratings and adjustable slits. A slit width of 10 μm and a 1200 line/mm grating were used which resulted in a resolution of about 1.5 eV at 530 eV. The absolute photon energy calibration of the monochromator was estimated to be accurate to 0.5 eV at 530 eV.

Apparatus 1 has been described previously.<sup>11</sup> Thus we will give only a brief description and mention some recent improvements. D<sub>2</sub>O films, typically hundreds of angstroms thick, were grown by condensing D<sub>2</sub>O vapor via a doser tube on an Al<sub>2</sub>O<sub>3</sub> substrate cooled to 20 K. After completion of the initial film growth, the surface was continuously refreshed by slow condensation of the

vapor from the doser tube at all times, while keeping the chamber pressure in the 10<sup>−10</sup>-Torr range. This technique was found to be essential to avoid surface contamination by the ambient at these low temperatures. Photodesorbed ions were detected by a set of microchannel plates and mass analyzed by a time-of-flight (TOF) method.<sup>5</sup> The TY signal was detected by a positively biased channeltron approximately 3 cm from the sample. Either signal was simultaneously normalized to the incident photon flux using the TY signal from a graphite-coated mesh positioned in the incident photon beam.

Measurements with apparatus 2 were carried out on the grasshopper monochromator of SSRL beam line I-1. The fixed 15-μm slits and the 1200 lines/mm holographic grating resulted in a resolution of about 2.5 eV at 530 eV. The apparatus has been described previously.<sup>1,25</sup> The H<sub>2</sub>O films were condensed via a needle doser onto a Ni(110) substrate at 90 K. The desorbing H<sup>+</sup> ions were detected by a TOF detector<sup>25</sup> and the TY signal from the sample was measured using a spiraltron electron multiplier. The simultaneous normalization to the incident photon flux and the monochromator transmission function was achieved by dividing the sample signals by the TY signal from an *in situ* Cu-coated metal grid.<sup>26</sup>

## III. RESULTS AND DISCUSSION

### A. Bulk and surface NEXAFS

In Fig. 1 we show the spectral yield of D<sup>+</sup>, which was the dominant ionic species, from solid D<sub>2</sub>O. Also shown are the TY measurements of the same sample and the gas-phase electron energy-loss spectrum (ELS) (Ref. 17) which is proportional to the absorption coefficient. While the ELS spectrum resolves at least four peaks below the gas-phase O(1s) ionization limit (539.7 eV) (Ref. 13), both

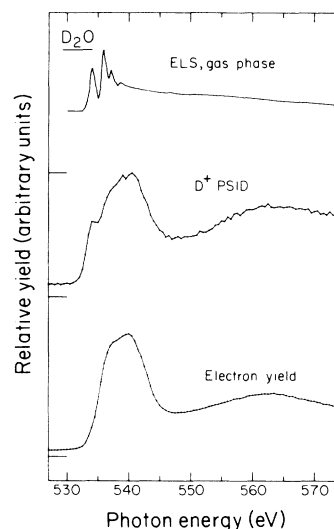


FIG. 1. Top: Electron energy-loss spectrum of water vapor (Ref. 17). Middle: D<sup>+</sup> photoion yield from D<sub>2</sub>O ice condensed at 20 K. Bottom: Total electron yield from D<sub>2</sub>O ice. The energy scales for the D<sub>2</sub>O ice results are estimated to be accurate to ±0.5 eV.

$D^+$  yield and TY signal exhibit a considerably broader peak structure with a maximum around 540 eV. The  $D^+$  yield exhibits an additional fine structure at the threshold which coincides with the first peak in the ELS spectrum but is missing in the TY signal.  $H^+$  PSID and TY measurements from ice condensed at 90 K gave virtually identical results. Recent work on condensed  $NH_3$  at 20 K (Ref. 16) and 90 K (Ref. 27) also shows agreement between the first peak of the corresponding ELS spectrum and the first near-edge fine-structure feature of the PSID yield. In contrast to  $D_2O$  ice, there is also a very weak low-energy shoulder in the TY signal of  $NH_3$  condensed at 20 K (Ref. 16) and 90 K.<sup>27</sup>

The sharp features observed in the gas-phase ELS spectrum are attributed to Rydberg transitions.<sup>17,28</sup> The first peak (Fig. 1) is due to a transition from the  $1s(1a_1)$  to a  $3s$ -derived orbital ( $3sa_1$ ), while the second and third peaks result from transitions to  $3p$ -like orbitals.<sup>29</sup>

We interpret the TY signal as representing the bulk photoabsorption coefficient.<sup>2</sup> Figure 1 shows that the Rydberg excitations observed in the gas phase are severely broadened in the solid and shifted to higher energy. A similar shift has been observed in the vacuum ultraviolet absorption.<sup>6,7</sup> The broadening is not explainable by the difference in the experimental resolution (ELS: 0.5 eV) (Ref. 17) but has to be of intrinsic nature related to the electronic interaction in the solid. A similar broadening has been observed in the O  $KVV$  Auger spectrum of solid  $H_2O$  (Ref. 12) and the O  $1s$  XPS line of ice which is twice as broad as in the gas phase.<sup>11</sup>

Condensation is expected to perturb the larger, more diffuse Rydberg orbitals. Table I shows the calculated radii for several Rydberg orbitals of the  $H_2O$  molecule.<sup>30</sup> In solid  $D_2O$ , the orbitals of one molecular unit should interact strongly with those of another since the oxygen-oxygen intermolecular distance (2.76 Å) is comparable to the Rydberg radii. This can account for the observed shifting and broadening of the Rydberg excitations in ice. In solid  $NH_3$ , the N-N distance (i.e., the intermolecular separation) is considerably longer (3.35 Å) (Ref. 31) suggesting a weaker interaction with the Rydberg states. This trend is confirmed by noting that the TY data of  $NH_3$  show a considerably closer comparison with the gas phase<sup>16</sup> than in the case of  $D_2O$ . Similar perturbations of Rydberg excitations upon condensation have also been observed in  $PH_3$  and  $SiH_4$ .<sup>32</sup>

We interpret the PSID yield spectrum as partly (see below and Ref. 27) reflecting the electronic structure of surface molecules in the outermost layer of the film. The reduced coordination of these molecules lowers the pertur-

bation of the Rydberg states. (The oxygen-oxygen distance of  $H_2O$  dimer is  $2.98 \pm 0.4$  Å.<sup>35</sup>) The lowest-energy peak of the PSID yield coincides with the first Rydberg ( $1s \rightarrow 3sa_1$ ) excitation observed in the gas phase,<sup>17</sup> while the higher-lying absorption features are shifted to higher energy and broadened as compared to the ELS spectrum, more closely resembling the TY or bulklike spectrum. This observation follows the trend in Rydberg orbital size (Table I), assuming the perturbation strength increases with increasing wave-function overlap. Another possible explanation for the "bulklike" portion of the PSID curve is based on the recently demonstrated phenomenon of x-ray-induced electron-stimulated ion desorption (XESD).<sup>27</sup> In the XESD process, secondary electrons produced by x-ray absorption in the bulk  $H_2O$  ice film cause desorption of ions from the surface. Such a process would tend to mimic the TY spectrum and thereby contribute an apparent broadening of the higher Rydberg excitations in the PSID curve. At this time, we have no way of distinguishing this secondary mechanism from the primary PSID process at the O  $K$  edge because the poorer resolution of the  $H_2O$  spectra does not allow a detailed XESD investigation as in the case of  $NH_3$ .<sup>27</sup> It is likely, however, that the situation in  $D_2O$  is similar to that in  $NH_3$ .

### B. Bulk EXAFS

In Fig. 2 we show the TY spectrum of  $H_2O$  ice, measured in apparatus 2, together with the EXAFS spectrum after background subtraction. The TY EXAFS spectrum was Fourier transformed in the range  $3.95 \leq k \leq 8.4$  Å<sup>-1</sup>. The phase shift was derived using standard techniques<sup>33</sup> assuming an oxygen-oxygen distance  $R^{O-O} = 2.76$  Å.<sup>34</sup>  $\phi^{O-O}(k)$  is the sum of the phase shifts occurring at the absorbing and at the backscattering oxygen atoms. The  $H^+$  PSID EXAFS spectrum was found to be similar to the TY spectrum. Owing to the likely XESD contribution<sup>27</sup> mentioned above, we did not pursue the EXAFS analysis of the PSID signal.

We found  $\phi^{O-O}(k)$  to be a linear function of  $k$  in the in-

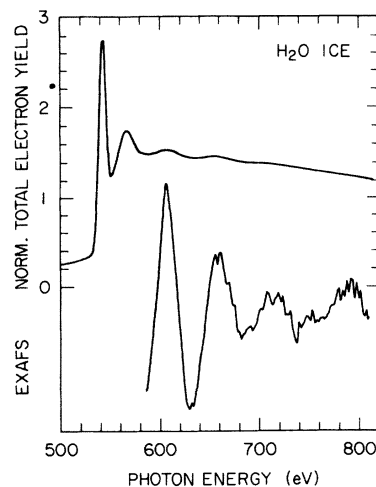


FIG. 2. Total photoelectron yield and background-subtracted photoelectron yield (EXAFS) from  $H_2O$  ice condensed at 90 K.

TABLE I. Rydberg-orbital radii for  $H_2O$  (from Ref. 30).

| Rydberg orbital | $\langle r^2 \rangle^{1/2}$ (Å) |
|-----------------|---------------------------------|
| $3sa_1$         | 2.21                            |
| $3pb_2$         | 2.56                            |
| $3pb_1$         | 3.65                            |
| $3pa_1$         | 3.91                            |

vestigated  $k$  range:

$$\phi^{O-O}(k) = 1.914 - 0.558k \quad (1)$$

This experimentally-derived phase shift is compared in Fig. 3 to the calculated curve by Teo and Lee<sup>22</sup> which can be written in parametrized form as

$$\phi^{O-O}(k) = 3.419 - 0.96k + 0.0256k^2 \quad (2)$$

The theoretical phase shift agrees very well with the experimentally-derived one and yields a distance which is within 0.02 Å of the known value (2.76 Å). It is noteworthy that this observation strongly supports a recent surface EXAFS analysis of oxygen on Al(111) (Ref. 20) in which the theoretical O-O phase shift by Teo and Lee<sup>22</sup> was used for the determination of the oxygen-oxygen distance.

#### IV. CONCLUSIONS

We present the first combined TY and PSID  $K$ -shell NEXAFS and EXAFS study of solid H<sub>2</sub>O and D<sub>2</sub>O. In comparison to the gas phase the low-lying Rydberg states of the water molecule were found to be severely broadened and shifted to higher energy in the TY spectrum of the solid state. The PSID NEXAFS spectra indicate a reduced Rydberg-state perturbation in the surface sites. Based on the known oxygen-oxygen distance in amorphous ice the EXAFS analysis of the TY spectrum yielded the total oxygen-oxygen scattering phase shift. The phase-shift calculation by Teo and Lee<sup>22</sup> agrees well with the experimentally-derived phase shift.

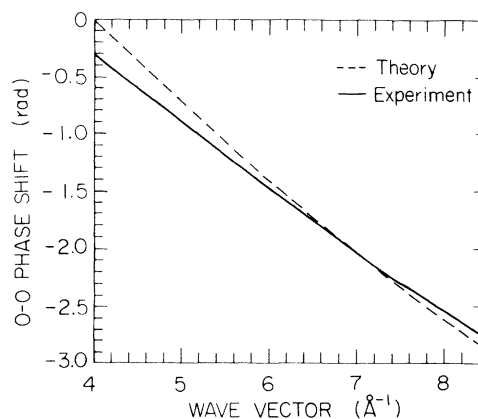


FIG. 3. Comparison of experimental and theoretical (Ref. 22) oxygen-oxygen phase shifts.

#### ACKNOWLEDGMENTS

This work was supported by the Naval Weapons Center Independent Research Fund, the U.S. Office of Naval Research, and the U.S. Department of Energy. Experiments were conducted at the Stanford Synchrotron Radiation Laboratory which is supported by the Department of Energy, Office of Basic Energy Sciences, the National Science Foundation, division of Materials Research, and the National Institutes of Health, Biotechnology Resource Program, Division of Research Resources.

\*Also at Stanford Synchrotron Radiation Laboratory, Stanford Linear Accelerator Center, Bin 69, P.O. Box 4349, Stanford, CA 94305 (mailing address).

†Present address: Hewlett-Packard Company, Deer Creek Laboratory, Palo Alto, California 94304.

<sup>1</sup>J. Stöhr, K. Baberschke, R. Jaeger, R. Treichler, and S. Brennan, *Phys. Rev. Lett.* **47**, 381 (1981); J. Stöhr and R. Jaeger, *Phys. Rev. B* **26**, 4111 (1982).

<sup>2</sup>A. Bianconi, *Appl. Surf. Sci.* **6**, 392 (1980).

<sup>3</sup>For a review, see E. A. Stern, *Contemp. Phys.* **19**, 289 (1978); D. R. Sandstrom and F. W. Lytle, *Ann. Rev. Chem.* **30**, 215 (1979); P. Eisenberger and B. M. Kincaid, *Science* **200**, 1441 (1978); P. A. Lee, P. H. Citrin, P. Eisenberger, and B. M. Kincaid, *Rev. Mod. Phys.* **53**, 769 (1981).

<sup>4</sup>A. P. Hitchcock and C. E. Brion, *J. Electron Spectrosc.* **18**, 1 (1980).

<sup>5</sup>M. L. Knotek, V. O. Jones, and V. L. Rehn, *Phys. Rev. Lett.* **43**, 300 (1979).

<sup>6</sup>M. Watanabe, I. Kitamura, and Y. Nakai, in *VUV Radiation Physics*, edited by E. E. Koch, R. Haensel, and C. Kunz (Perгамon, Berlin, 1974), p. 70.

<sup>7</sup>T. Shibaguchi, H. Onuki, and R. Onaka, *J. Phys. Soc. Jpn.* **42**, 152 (1974).

<sup>8</sup>M. J. Campbell, J. Liesegang, J. D. Riley, R. C. G. Leckey, J. G. Jenkin, and R. T. Poole, *J. Electron Spectrosc. Relat. Phenom.* **15**, 83 (1979).

<sup>9</sup>R. A. Rosenberg, V. Rehn, V. O. Jones, A. K. Green, C. C.

Parks, G. Loubriel, and R. H. Stulen, *Chem. Phys. Lett.* **80**, 488 (1981).

<sup>10</sup>B. Baron and F. Williams, *J. Chem. Phys.* **64**, 3896 (1974).

<sup>11</sup>K. Siegbahn, C. Nordling, G. Johansson, J. Hedman, P. F. Heden, K. Hamrin, U. Gelius, T. Bergmark, L. O. Werme, R. Manne, and Y. Baer, *ESCA Applied to Free Molecules* (North-Holland, Amsterdam, 1969).

<sup>12</sup>R. R. Rye, T. E. Madey, J. E. Houston, and P. H. Holloway, *J. Chem. Phys.* **69**, 1504 (1978).

<sup>13</sup>G. P. Parravicini and L. Resca, *Phys. Rev. B* **8**, 3009 (1973).

<sup>14</sup>*Desorption Induced by Electronic Transitions, DIET-I*, edited by N. H. Tolk, M. M. Traum, J. C. Tully, and T. E. Madey (Springer, Berlin, 1982).

<sup>15</sup>D. E. Ramaker, in Ref. 14.

<sup>16</sup>R. A. Rosenberg, V. Rehn, A. K. Green, P. R. LaRoe, and C. C. Parks, in Ref. 14.

<sup>17</sup>G. R. Wight and C. E. Brion, *J. Electron Spectrosc. Relat. Phenom.* **4**, 25 (1974).

<sup>18</sup>B. Lamb, in *Physics and Chemistry of Ice*, edited by E. Whalley, S. J. Jones, and L. W. Gold (Royal Society of Canada, Ottawa, 1973).

<sup>19</sup>D. Norman, S. Brennan, R. Jaeger, and J. Stöhr, *Surf. Sci.* **105**, L297 (1981).

<sup>20</sup>J. Stöhr, L. I. Johansson, S. Brennan, M. Hecht, and J. N. Miller, *Phys. Rev. B* **22**, 4052 (1980).

<sup>21</sup>J. Stöhr, R. Jaeger, and T. Kendelewicz, *Phys. Rev. Lett.* **49**, 142 (1982).

- <sup>22</sup>Boon-Keng Teo and P. A. Lee, *J. Am. Chem. Soc.* **101**, 2815 (1979).
- <sup>23</sup>P. A. Lee and G. Beni, *Phys. Rev. B* **15**, 2862 (1977).
- <sup>24</sup>J. Stöhr and R. Jaeger (unpublished).
- <sup>25</sup>R. Jaeger, J. Stöhr, J. Feldhaus, S. Brennan, and D. Menzel, *Phys. Rev. B* **23**, 2102 (1981).
- <sup>26</sup>J. Stöhr, R. Jaeger, J. Feldhaus, S. Brennan, D. Norman, and G. Apai, *Appl. Opt.* **19**, 3911 (1980).
- <sup>27</sup>R. Jaeger, J. Stöhr, and T. Kendelewicz (unpublished).
- <sup>28</sup>G. H. F. Diercksen, W. P. Kraemer, T. N. Rescigno, C. F. Bender, B. V. McKoy, S. R. Langhoff, and P. W. Langhoff, *J. Chem. Phys.* **76**, 1043 (1982).
- <sup>29</sup>This assignment has been challenged by H. T. Wang, W. S. Fels, and S. P. McGlynn, *J. Chem. Phys.* **67**, 2614 (1977).
- <sup>30</sup>W. A. Goddard III and W. J. Hunt, *Chem. Phys. Lett.* **24**, 464 (1974).
- <sup>31</sup>J. W. Reed and P. M. Harris, *J. Chem. Phys.* **35**, 1730 (1961).
- <sup>32</sup>E. E. Koch and B. F. Sonntag, *Synchrotron Radiation Techniques and Applications* (Springer, Berlin, 1979), p. 304.
- <sup>33</sup>J. Stöhr, R. Jaeger, and S. Brennan, *Surf. Sci.* **117**, 503 (1982).
- <sup>34</sup>S. W. Peterson and H. A. Levy, *Acta Crystallogr.* **10**, 70 (1957); M. Blackman and N. D. Lisgarten, *Proc. R. Soc. London Ser. A* **239**, 93 (1957).
- <sup>35</sup>T. R. Dyke and J. S. Muentzer, *J. Chem. Phys.* **60**, 2929 (1974).